Journal of Chromatography, 284 (1984) 33–51
Elsevier Science Publishers B.V., Amsterdam — Printed in The Netherlands

CHROM. 16,318

CHROMATOGRAPHIC STUDY OF THE THERMODYNAMIC AND KINETIC CHARACTERISTICS OF SILICA-BOUND CONCANAVALIN A

AMY J. MULLER and PETER W. CARR*
University of Minnesota, Department of Chemistry, Minneapolis, MN 55455 (U.S.A.)
(First received February 22nd, 1983; revised manuscript received September 22nd, 1983)

SUMMARY

A method has been developed for determining the rate constants for dissociation of sugar derivatives from silica-immobilized concanavalin A using high-performance liquid affinity chromatography. The rate constants observed are *ca.* ten-fold smaller than those reported in solution. Using 10-μm silica particles, it has been shown that slow dissociation of the sample from the immobilized affinity ligand is the predominant factor responsible for the large plate heights observed in this system. The effect of several chromatographic variables (temperature, mobile phase modifiers and particle size) on the observed dissociation rate constant and peak centroid have been evaluated.

INTRODUCTION

High-performance liquid affinity chromatography (HPLAC) is a relatively new technique of biochemical analysis which combines the high-speed characteristics of high-performance liquid chromatography (HPLC) with the inherent selectivity of biospecific interactions[1,2]. Several HPLAC systems have recently been reported including the separation of proteases using silica-bound soybean trypsin inhibitor[3], various enzymes with silica-bound triazine dyes[4], antigens with silica-immobilized antibodies[5], and glycoproteins with silica-bound concanavalin A[6]. The large effect of pore size on the efficiency of HPLAC separations has recently been investigated[7]. In most instances, the observed plate heights (H) are much larger (*ca.* 2 mm) than those normally encountered in HPLC of small molecules at comparable flow-rates on columns packed with similar particle and pore size. For this reason it may be premature to refer to these methods as high-performance techniques, but the term is already well established and will be used here. The reason for the increased plate height in HPLAC has been attributed to slow sample dissociation from the biospecific adsorbent[3,6].

The bioselective ligand chosen for this investigation, concanavalin A, is a saccharide-binding globular protein (mol.wt. 102,000) used extensively for the characterization of cell surfaces via the techniques of cell agglutination and quantitative labelling[8]. Both direct concanavalin A precipitation and concanavalin A affinity

0021-9673/84/$03.00

chromatography have been used to isolate and purify polysaccharides, glycoproteins, and membrane components. The structural and physical properties, as well as the solution phase monosaccharide binding behavior of concanavalin A, have been extensively studied[9]. The choice of concanavalin A for this investigation was, therefore, based primarily upon its general analytical utility for biochemical separations and the availability of solution phase binding parameters.

In this paper, we report on the use of a method which can be used to estimate the dissociation rate constants characterizing the interaction between biospecific ligands and chromatographic solutes using HPLAC. The calculation of the dissociation rate constant (k_d) is based on the approach presented by Horváth and Lin[10]. According to their model, the observed plate height (H) can be separated into four independent contributions,

$$H_{\text{total}} = H_{\text{dispersion}} + H_{\text{ext.diff.}} + H_{\text{int.diff.}} + H_{\text{kinetic}} \tag{1}$$

The term $H_{\text{dispersion}}$ accounts for the plate height increment due to axial dispersion of the sample in the interstitial space and is given by

$$H_{\text{dispersion}} = \frac{2\lambda D_M}{U_e} + \frac{2\gamma d_p U_e^{1/3}}{U_e^{1/3} + \omega(D_M/d_p)} \tag{2}$$

where λ, γ and ω are structural parameters of the column packing, D_M is the solute diffusion coefficient, d_p is the particle diameter and U_e is the interstitial linear velocity. The plate height contribution, $H_{\text{ext.diff.}}$, is due to "film" resistance at the particle boundary and is given by

$$H_{\text{ext.diff.}} = \frac{\kappa(k_0 + k' + k_0k')^2 d_p^{5/3} U_e^{2/3}}{(1 + k_0)^2(1 + k')^2 D_M^{2/3}} \tag{3}$$

where κ is an additional structure packing factor, k_0 is the ratio of intraparticle void volume to interstitial void volume, and k' is the solute's capacity factor. The intraparticle diffusion resistance to mass transfer is given by

$$H_{\text{int.diff.}} = \frac{\theta(k_0 + k' + k_0k')^2 d_p^2 U_e}{30 D_M k_0 (1 + k_0)^2 (1 + k')^2} \tag{4}$$

for spherical particles where θ is the internal tortuosity factor. H_{kinetic} is the plate height contribution due to slow (chemical) kinetic processes and is given equivalently by

$$H_{\text{kinetic}} = \frac{2k' U_e}{(1 + k_0)(1 + k')^2 k_d} = \frac{2k'^2 U_e}{(1 + k_0)(1 + k')^2 \varphi k_a} \tag{5}$$

where φ is the phase ratio (moles of bioactive sites expressed with the volume of the mobile phase in the column), k_a is the association rate constant for binding of the solute in consistent units and k_d is the dissociation rate constant for the reverse process. Note that H_{kinetic} is the only plate height contribution which does not depend

on particle diameter. We have applied these equations to study the kinetics of the interaction between silica-bound concanavalin A and several sugar derivatives. Recently, Chen and Weber[11] have derived the above equations from the viewpoint of the Giddings random walk model[12]. We believe that they are sufficiently well founded, at least theoretically, to use them as the basis for measurement of k_a and k_d.

EXPERIMENTAL

Materials

Concanavalin A (Con A, Type IV), *p*-nitrophenyl-α-D-mannopyranoside (pNp-mannoside), *p*-nitrophenyl-α-D-glucopyranoside (pNp-glucoside), *p*-nitrophenyl-β-D-galactopyranoside (pNp-galactoside), and α-methyl-D-mannoside (Grade III, αMDM) were used as purchased from Sigma (St. Louis, MO, U.S.A.). Fractosil 500 (pore diameter, 420 Å; particle diameter, 40–60 μm) was obtained from E. Merck (Darmstadt, F.R.G.) and washed with concentrated nitric acid prior to use. LiChrospher 500 (Batch No. YE 496; pore diameter, 500 Å; particle diameter, 10 μm) was also obtained from E. Merck. γ-Aminopropyltrimethoxysilane was obtained from Silar (Scotia, NY, U.S.A.). All other chemicals were reagent grade.

Preparation of biospecific adsorbants

Con A was coupled to both Fractosil 500 and LiChrospher 500 by the same method (Fig. 1). The porous silica was first aminosilanized. Silica (3 g) was suspended in 30 ml of distilled water and added to 1 ml of γ-aminopropyltrimethoxysilane dissolved in 10 ml of distilled water. The resulting suspension was ultrasonically vacuum degassed and vigorously shaken for 20 min. The supernatant was immediately filtered off and the silica was dried at 55°C for 24 h and then at 85°C for 24 h under atmo-

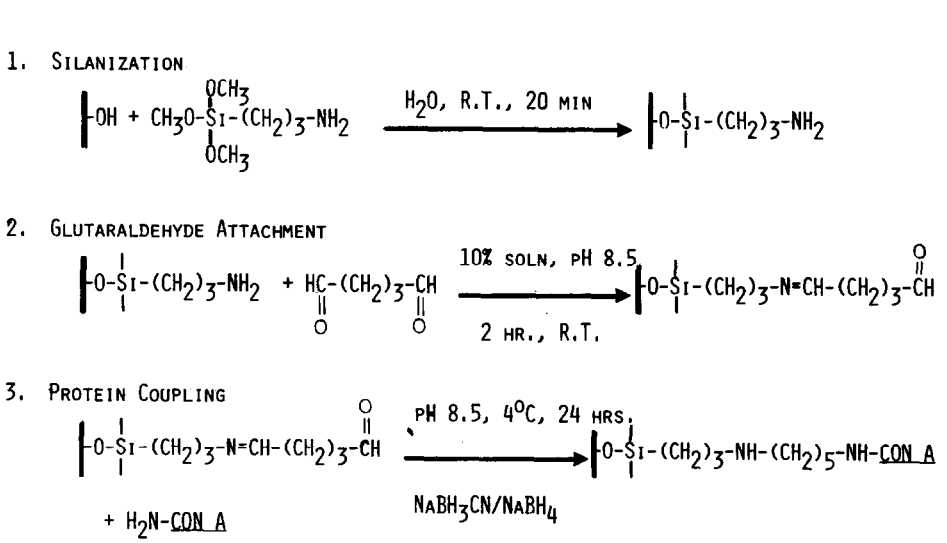

Fig. 1. Scheme for the immobilization of concanavalin A on microparticulate silica.

spheric pressure[13]. Con A was immobilized on the aminosilanized silica by the glutaraldehyde method[14]. To 2.8 g of aminosilanized silica were added 40 ml 10% (v/v) glutaraldehyde in 0.1 *M* sodium phosphate buffer, pH 8.5. The suspension was ultrasonically agitated and vacuum degassed at room temperature for 1 h and then allowed to react at room temperature and pressure with occasional swirling for 1 h. The silica suspension was then poured onto a sintered glass funnel and washed first with 1500 ml of distilled water and then with 250 ml of the protein coupling buffer (0.1 *M* borate, 0.5 *M* sodium chloride, 0.01 *M* magnesium chloride, 0.001 *M* calcium chloride, pH 8.5). The glutaraldehyde-modified carrier was suspended in 20 ml of Con A solution in the protein coupling buffer (5 mg Con A/ml) and allowed to react at room temperature for 1 h and additionally for 24 h at 4°C. The Con A–silica suspension was filtered and then washed with coupling buffer until the filtrate had negligible absorbance at 280 nm. Finally, the Con A–silica was reduced with sodium cyanoborohydride[15] (5 mmole in 50 ml of coupling buffer, 3 h, room temperature) and then with sodium borohydride (2 mmole in 50 ml of coupling buffer, 1 h, room temperature). The silica was washed with the appropriate mobile phase and stored at 4°C. The amount of Con A bound to the silica was determined by the difference in absorbance of the Con A solution at 280 nm before and after immobilization. The amount of Con A detected in the washings of the silica was included in this determination. The amount of Con A bound to the silica (in milligrams of Con A per gram of silica) was found to be 37.6 mg/g for Fractosil 500 and 26.9 mg/g for LiChrospher 500.

More recently, we purified commercial Con A prior to immobilization by the method of Cunningham *et al.*[16] to isolate the intact subunits and provide a more homogeneous material. Although the yield of biological binding activity on the glass support was improved from 50% to *ca.* 98%, the kinetic properties of the material were not significantly altered.

Column packing and chromatographic conditions

The 10-μm separation columns (5 cm × 0.5 cm I.D.) were slurry packed at 3000 p.s.i. using 2 m*M* αMDM in distilled water as the suspending medium and the stirred upward packing method[17]. The 50-μm particles were manually slurry packed into 5 cm × 0.3 cm I.D. glass columns. An HPLC system comprised of a high-pressure pump (Altex), an injector (Valco) fitted with either a 10 ml (for isotherm measurements) or 25-μl loop, and a UV–visible spectrophotometer (Hitachi) equipped with 10-μl flow cell (Altex) was used. Column jackets were used and temperature control (± 1°C) was provided by a thermostated water circulator (Haake, Model FE). The detection wavelengths for nitrophenyl sugars was 305 nm. The mobile phase used was 0.02 *M* sodium phosphate, pH 6.0 containing 0.5 *M* sodium chloride, 0.01 *M* magnesium chloride, and 0.001 *M* calcium chloride, proposed stabilizers of Con A. The column dead volume was measured using methanol. The data collection system consisted of a d.c. amplifier (Keithley Instruments, Cleveland, OH, U.S.A.) and an Apple II Plus computer equipped with the ADALAB System (Interactive Microware, State College, PA, U.S.A.).

Isotherm measurements

The binding isotherms for pNp-mannoside and pNp-glucoside on the Fractosil

500 column were measured by the break-through method[18]. Using a 10-ml injection loop, a known concentration of sugar solution was injected onto the column. The rise from baseline was nearly vertical and thus it makes little difference whether one uses the point of initial departure from baseline or the point of establishment of the new steady state condition to calculate the amount of sugar adsorbed (see Fig. 5b). The amount of sugar adsorbed on the silica was determined from the breakthrough volume corrected for the dead volume. The stationary phase concentration, C_s, was then calculated using eqn. 6,

$$C_s = [(V_b - V_0)C_m]/n_C \tag{6}$$

where V_b is the breakthrough volume, V_0 is the column dead volume, C_m is the concentration of sugar in the mobile phase, and n_C is the total number of moles of Con A in the column. The procedure assumes that all bound Con A is biochemically active. Since non-binding sugars are essentially unretained on these columns, we believe that the adsorption process is accounted for completely by bioselective adsorption on Con A and that non-specific adsorption to the support is negligible.

Calculation of elution parameters

Because the chromatographic peaks obtained exhibited severe tailing (see Fig. 2), simple measurement of the volume at peak maximum could not be used as a thermodynamically valid measure of sugar retention. Similarly, under these conditions, the peak width at half maximum could not be used to obtain the true peak variance using the conventional Gaussian peak formulae. To circumvent these difficulties, an on-line data acquisition system was used. The 10-mV detector signal was amplified 100-fold using a detector time constant setting of 0 and an amplifier rise time of 0.5 sec. The data acquisition rate was adjusted from 0.5 sec/point for the narrowest peaks up to 3 sec/point for the widest peaks so that an average of 100 data points were collected across each peak. A total of *ca.* 300 points were taken for each chromatographic run so that an accurate estimation of the baseline could be made. The end of the peak was first estimated by visual inspection of the recorder trace and then by inspecting the data acquired and determining the point at which the data points were changing by less than 1.0%. In all cases, the signal/noise at peak maximum was better than 200. Baseline subtraction was performed on each peak. The average of the ten points prior to the start of the peak and the average of the ten points after the end of the peak were computed. The line connecting these two averages was determined and subtracting from the data set. The zeroth, first, and second moments were then calculated using the standard definitions of the normalized central moments[19]:

$$\mu_0' \equiv \int_0^\infty C(t)\mathrm{d}t \tag{7}$$

$$\mu_1' \equiv 1/\mu_0 \int_0^\infty tC(t)\mathrm{d}t \tag{8}$$

$$\mu_2' \equiv 1/\mu_0 \int_0^\infty (t - \mu_1)^2 C(t)\mathrm{d}t \tag{9}$$

where μ'_0, μ'_1, and μ'_2 are the zeroth, first, and second normalized central moments, respectively, and $C(t)$ is the concentration at time t during peak elution. These definitions were translated into the following formulae in this study:

$$\mu'_0 = \Sigma H(t) \tag{10}$$

$$\mu'_1 = \frac{\Sigma H(t) \cdot t}{\Sigma H(t)} \tag{11}$$

$$\mu'_2 = \frac{\Sigma H(t) \cdot t^2}{\Sigma H(t)} - \mu'^2_1 \tag{12}$$

where $H(t)$ is the peak height at time t, during peak elution. The summations were calculated over the interval previously defined by the peak starting and peak ending points. The plate height, H, was then computed as:

$$H = \frac{\mu'_2 L}{\mu'^1_1} \tag{13}$$

where L is the length of the column.

RESULTS AND DISCUSSION

Bioselective interaction

The main import of this series of experiments was to demonstrate that the biochemical selectivity of Con A is not seriously altered by immobilization on silica gel. The Con A packings prepared were first evaluated with respect to their ability to resolve a mixture of closely related sugar derivatives. The *p*-nitrophenyl derivatives were chosen because they are easily detected at low concentration at a wavelength of 305 nm. Fig. 2 shows typical sugar separations on the 10-μm and 50-μm columns. The three sugars are well resolved on both columns, although the resolution is better on the smaller diameter packing material, as expected. In contrast to conventional HPLC, the improvement in H is definitely not in proportion to the decrease in the square of the particle diameter. The elution order of these sugars is the same as their relative Con A binding affinities as determined by solution phase studies[20].

As a further test of biospecific interaction, the effect of a competing sugar (αMDM) on the elution volume of pNp-mannoside was determined. The effect of competing sugar can be modeled by assuming that the binding constants of both S_1 (pNp-mannoside) and S_2 (αMDM) are independent and that a Con A monomer can bind only one sugar. The above reactions translate into the following equilibrium expressions:

$$K_1 = [\text{Con A:S}_1]_s/[\text{Con A}]_s[\text{S}_1]_m \tag{14}$$

$$K_2 = [\text{Con A:S}_2]_s/[\text{Con A}]_s[\text{S}_2]_m \tag{15}$$

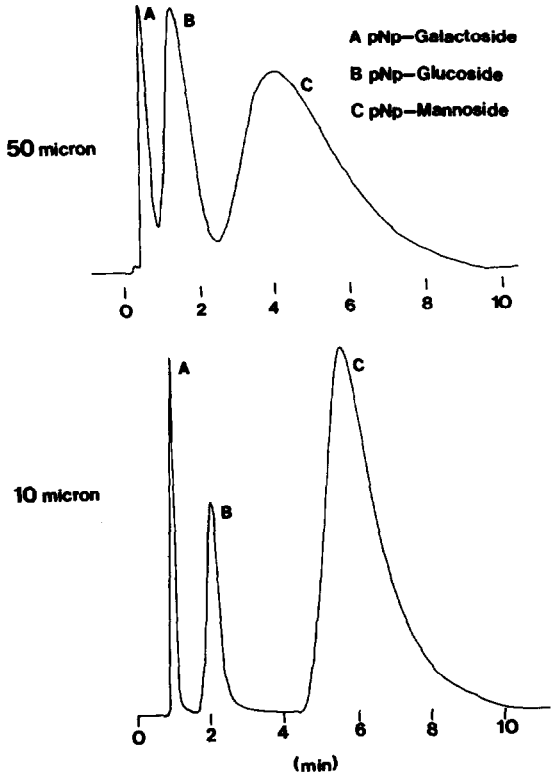

Fig. 2. Separation of sugar derivatives. Mobile phase: pH 6.0, 0.02 *M* sodium phosphate, 0.5 *M* sodium chloride, 0.01 *M* magnesium chloride, 0.001 *M* calcium chloride. Flow-rate: 1 ml/min. Sample: 25 μl containing *ca.* 0.5 μg of pNp-galactoside (A), 1.2 μg of pNp-glucoside (B), 5.0 μg of pNp-mannoside (C). Column a: 5.0 × 0.3 cm I.D.; 38 mg of Con A per gram of silica; 50 μm; nominal pore size, 420 Å. Column b: 5.0 × 0.5 cm I.D.; 27 mg of Con A per gram of silica; 10 μm; nominal pore 500 Å.

where the subscripts s and m indicate the stationary and mobile phases, respectively. Mass balance considerations lead to the following three conservation expressions:

$$N^0_{CA} = V_s([\text{Con A}]_s + [\text{Con A:S}_1]_s + [\text{Con A:S}_2]_s) \tag{16}$$

$$N^0_{S_1} = V_s([\text{Con A:S}_1]_s) + V_m([S_1]_m) \tag{17}$$

$$N^0_{S_2} = V_s([\text{Con A:S}_2]_s) + V_m([S_2]_m) \tag{18}$$

where N^0_{CA}, $N^0_{S_1}$, and $N^0_{S_2}$ are the total number of moles of Con A, S_1, and S_2. The parameters V_s and V_m are the volumes of the stationary and mobile phases, respectively. Since we are primarily concerned with the variation in retention of S_1 as a function of the concentration of S_2 in the eluent, the capacity factor, k', for S_1 is needed. By the usual definition of k' as the mole fraction equilibrium constant and based on the assumption that only a small amount of S_1 is present compared to the

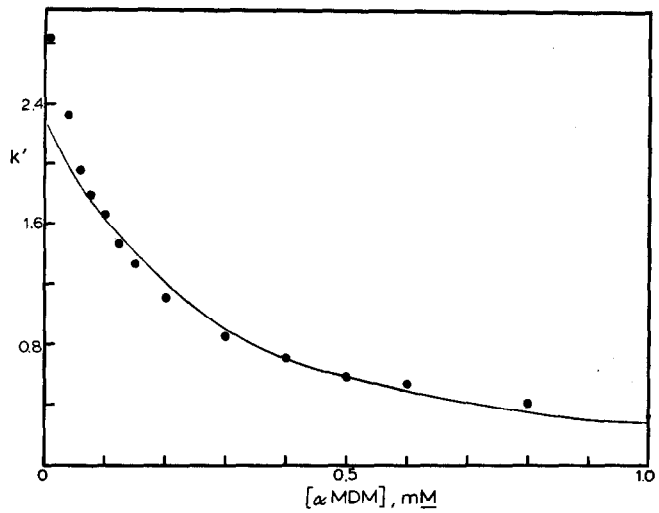

Fig. 3. Comparison of experimentally obtained k' (●), with the equilibrium binding model predictions (———). Column: 15 × 0.3 cm I.D.; 17 mg of Con A per gram of silica; 50 μm; nominal pore size, 420 Å. Mobile phase: pH 5.5, 0.02 *M* sodium acetate, 0.1 *M* sodium chloride, 0.001 *M* manganous chloride, 0.001 *M* calcium chloride. Flow-rate: 1 ml/min. Solute: 25 μl of 1.0 m*M* pNp-mannoside. The predicted k' values were calculated using eqn. 19 with $K_1 = 1.6 \cdot 10^4$, $K_2 = 0.76 \cdot 10^4$, $V_m = 0.85$ ml, and $N^0_{CA} = 1.57 \cdot 10^{-7}$.

available quantity of Con A binding sites (*i.e.* $N^0_{S_1} \ll N^0_{CA}$), the following equation is easily obtained:

$$k' = \frac{K_1 N^0_{CA}}{V_m(1 + K_2[S_2]_m)} \tag{19}$$

The effect of varying the concentration of S_2 on the k' value of S_1 is shown in Fig. 3. The column used for this single experiment was prepared by a somewhat different procedure than that described earlier and the amount of Con A bound to the silica was less than the amount bound via the glutaraldehyde procedure. Also, in this case, the k' value was estimated from the peak maximum rather than from the first peak moment. The concentration of S_1 injected in this experiment, 1.0 m*M*, is rather high and lies in the region of isotherm non-linearity (see Figs. 4 and 5). A more thermodynamically valid measurement would necessitate the use of a much less concentrated sugar solution to approach the region of isotherm linearity. However, it is experimentally impossible to detect pNp-mannoside at concentrations in the "linear" region of the isotherm.

The k' values shown in Fig. 3 decrease as expected from eqn. 19. The solid curve was fitted using a Simplex non-linear least squares method. The amount of active Con A on the column, N^0_{CA}, was obtained from the measurement of the weight of total Con A on the column and from the isotherm measurements (see below). The first two data points were excluded in determining the fitting parameters. The fitting parameters are $K_1 = 1.6 \cdot 10^4\ M^{-1}$ and $K_2 = 0.76 \cdot 10^4\ M^{-1}$ and are in good agreement with solution phase binding constants, despite the fact that we were esti-

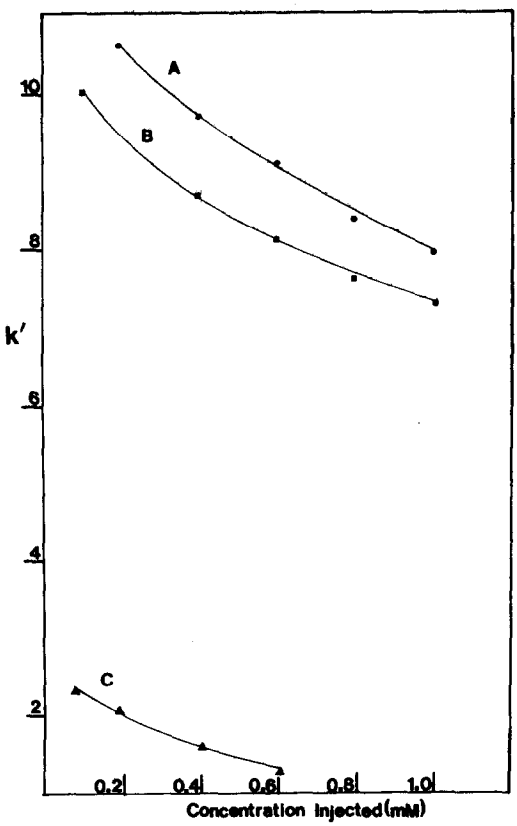

Fig. 4. Variation of k' with concentration of injected sugar. Mobile phase: pH 6.0, 0.02 *M* sodium phosphate, 0.5 *M* sodium chloride, 0.01 *M* magnesium chloride, 0.001 *M* calcium chloride. Flow-rate: 1 ml/min. Volume injected: 25 μl. (A) pNp-Mannoside on 50-μm particles, (B) pNp-Mannoside on 10-μm particles. (C) pNp-Glucoside on 10-μm particles.

mating k' from the position of peak maximum and were operating at sample concentrations in the non-linear isotherm region. When the experiment was performed using the glutaraldehyde-immobilized Con A and the moments analysis method described earlier to calculate k', the fitting parameters were found to be $K_1 = 1.5 \cdot 10^4$ M^{-1} and $K_2 = 0.73 \cdot 10^4$ M^{-1}.

Thus, even though the association constants obtained by this chromatographic method are not rigorously "thermodynamic" parameters, the agreement with solution phase parameters indicates that the behavior of immobilized Con A is very similar to the behavior of soluble Con A in terms of the binding of S_1 and S_2. The data indicate poorest fit at concentrations of competing sugar, S_2, lower than 0.04 m*M*. At this time, we have no conclusive explanation for the results, but preliminarily we believe that the poor fit may be related to the heterogeneity of the binding sites (see isotherm studies), in particular to the existence of a small number of "strong" sites.

Galactose, a sugar which does not bind to Con A in solution[21], had *no* effect on the retention of pNp-mannoside when added to the mobile phase. Small organic

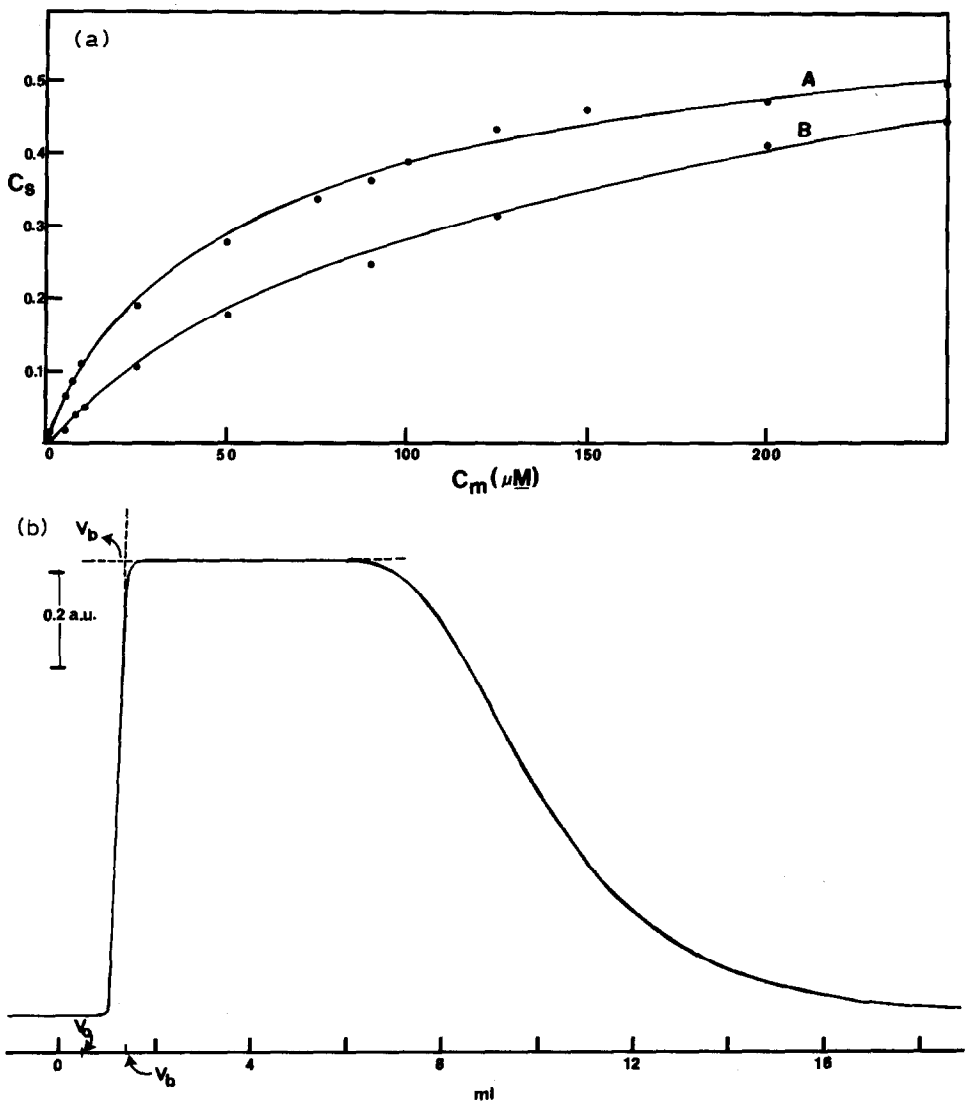

Fig. 5. (a) Distribution isotherms of pNp-mannoside (A) and pNp-glucoside (B) on Con A column. Column: 5.0 × 0.3 cm I.D.; 38 mg of Con A per gram of silica; 50 μm; nominal pore size, 420 Å. Mobile phase: pH 6.0, 0.02 *M* sodium phosphate, 0.5 *M* sodium chloride, 0.01 *M* magnesium chloride, 0.001 *M* calcium chloride. Flow-rate: 1 ml/min. C_s calculated using eqn. 6. (b) Typical breakthrough curve for isotherm measurement; V_0 = column dead volume, V_b = breakthrough volume (see eqn. 6); 10 ml of 0.075 m*M* pNp-mannoside injected.

molecules, such as nitrobenzene, chosen to emulate the nitrophenyl part of the sugar, elute near the void volume of these Con A columns indicating that non-bioselective interactions are negligible. We also noted that the peak widths and shapes of non-binding solutes are much better than the broad and asymmetric peaks obtained for pNp-mannoside (see Fig. 2), a solute which binds to Con A.

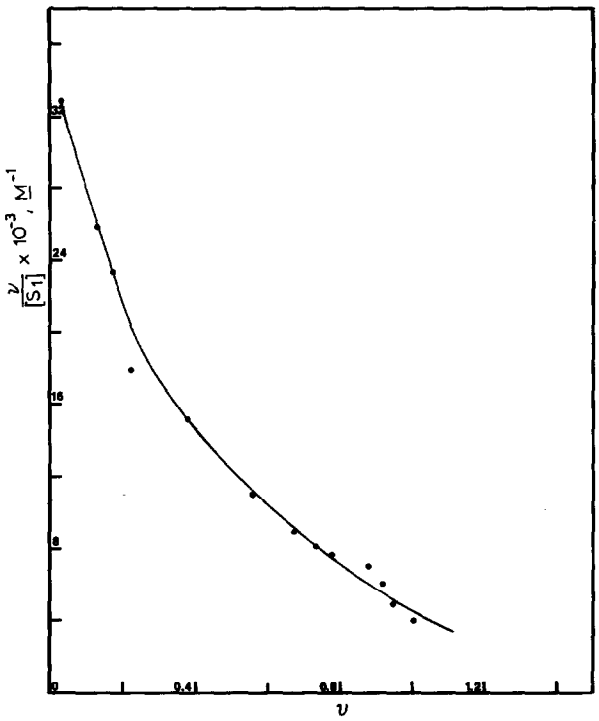

Fig. 6. Scatchard plot for the binding of pNp-mannoside to immobilized Con A. Column: 5.0 × 0.3 cm I.D.; 38 mg of Con A per gram of silica; 50 μm; nominal pore size, 420 Å. [S_1] = concentration of unbound pNp-mannoside, ν = number of moles of bound pNp-mannoside/number of moles of active Con A. All data taken from distribution isotherm of Fig. 5a.

Distribution isotherms

The elution volumes of the sugar derivatives on these Con A columns are strongly dependent on the concentration injected (Fig. 4). While plots of concentration injected *versus* peak area are linear over the range 10^{-5} *M* to 10^{-3} *M*, plots of concentration injected *versus* peak height are not linear. The distribution isotherms of pNp-mannoside and pNp-glucoside on Fractosil Con A are shown in Fig. 5a. Both isotherms are non-linear even at low concentrations and this non-linearity is responsible for the concentration dependent elution behavior observed. The distribution isotherm of pNp-mannoside as computed from eqn. 6 reaches a plateau at approximately C_s equal to 0.5, indicating that the immobilized Con A is approximately 50% active. The pNp-glucoside achieves a final value of C_s equal to 0.44.

The interaction of proteins with many species is often investigated by means of the so-called Scatchard plot[22]. In the present context, this translates into a plot of $\nu/[S_1]$ *vs.* ν where ν is defined as the ratio of the number of moles of bound S_1 to the number of moles of available Con A binding sites. When a single type of non-interacting binding site is present, the variables are related as follows:

$$\frac{\nu}{[S_1]} = \frac{n}{K} - \frac{\nu}{K} \tag{20}$$

TABLE I

EFFECT OF PARTICLE DIAMETER ON PLATE HEIGHT CONTRIBUTIONS

Mobile phase: pH 6.0, 0.02 *M* sodium phosphate, 0.5 *M* sodium chloride, 0.01 *M* magnesium chloride, 0.001 *M* calcium chloride. Solute: 25 μl of pNp-mannoside. Flow-rate: 1 ml/min.

Concentration injected (mM)	d_p = 10 μm*				d_p = 50 μm**			
	k'	H_{total} (mm)***	$H_{non\text{-}binding}$ (mm)§	$H_{kinetic}$ (mm)§§	k'	H_{total} (mm)***	$H_{non\text{-}binding}$ (mm)§	$H_{kinetic}$ (mm)§§
0.1	10.0	0.80	0.12	0.68	11.4	4.05	2.44	1.61
0.2	9.5	0.82	0.12	0.70	10.6	4.28	2.42	1.86
0.4	8.6	1.12	0.12	1.06	9.7	5.40	2.41	2.99

* Column: 5.0 × 0.5 cm I.D.; 27 mg Con A per gram silica; nominal pore size, 500 Å.

** Column: 5.0 × 0.3 cm I.D.; 38 mg Con A per gram silica; nominal pore size, 420 Å.

*** Calculated using eqn. 13.

§ Calculated using eqns. 2–4 with $k_0 = 0.6$, $\gamma = 0.6$, $\lambda = 7.5$, $\omega = 2.7$, $\theta = 1.0$, $\kappa = 0.17$ and $D_m = 0.45 \cdot 10^{-5}$ cm²/sec.

§§ $H_{kinetic} = H_{total} - H_{non\text{-}binding}$ (eqn. 21).

where $[S_1]$ is the concentration of unbound S_1. thus, a plot of $v/[S_1]$ *versus* v will have a slope of $-1/K$, where K is the equilibrium dissociation constant of the complex. The intercept on the $v/[S_1]$ axis will be equal to n/K, where n is the number of binding sites on a Con A monomer. As shown in Fig. 6, we do not observe a linear Scatchard plot for the binding of pNp-mannoside to Con A. This is consistent with a heterogeneous population of binding sites[23]. If there is more than one class of binding site the curve will be concave upwards as in Fig. 6. The points near $v = 0$ can be used to estimate the equilibrium binding constant of the strongest sites. Calculations of the asymptotic slope near $v = 0$ yields a binding constant of $7.6 \cdot 10^4\ M^{-1}$. This is significantly larger than the "average" binding constant ($1.6 \cdot 10^4\ M^{-1}$) determined from the equilibrium binding calculations (see Fig. 3). Although the Scatchard method has never been applied to the binding of pNp-mannoside to Con A in solution, Scatchard plots constructed for the binding of methyl-α-D-glucopyranoside[24] and methyl-α-D-mannapyranoside[25] to soluble Con A are linear over the pH range 5 to 7.3.

One possible source of binding site heterogeneity is the pH-dependent dimer–tetramer association of the Con A monomers[26]. At pH 6, Con A should exist predominantly in the tetramer form, though some dimers will be present. The immobilization procedure itself, as well as the complex surface of silica is probably responsible for some heterogeneity in the Con A binding sites. Each Con A monomer contains twelve lysine residues which are available for covalent attachment to the glutaraldehyde-derivatized silica. Therefore, it is unlikely that each Con A monomer is attached to the surface by the same number of linkages. In all subsequent experiments, the lowest concentrations of sugar detectable were injected to minimize the effects of isotherm non-linearity on the observed plate heights.

Evaluation of kinetic parameters

The plate heights obtained for sugar derivatives injected onto the Con A columns were much larger (*ca.* 0.1 cm) than those normally encountered in HPLC on 10-μm particles. The reduced plate height ($h = H/d_p$) were generally *ca.* 100, which grossly exceeds values for small molecules using HPLC. Our results with a non-binding, but structurally similar, sugar (*i.e.* pNp-galactose) indicate h values of only 12. By far, the most important contribution to plate height in this system is the effect of slow kinetic binding processes and not column packing inhomogeneity.

There are *two* distinct kinetic processes involved in Con A chromatography. The first is simple mass transfer resistance which may be predominantly in the flowing or stagnant mobile phase. In any case, mass transfer resistances and their contributions to H are proportional to some power of the particle diameter (see eqns. 2–4). As mentioned previously, we observed very little improvement in resolution upon changing the particle diameter from 50 to 10 μm. As shown in Table I, the total H on 10-μm and 50-μm particles differ by only a factor of 5 at the lowest sample concentration. Recently, Horváth and Lin[10] have described a kinetic contribution to H which does not depend on particle size, namely the chemical rate of association and dissociation of the solute from the stationary phase adsorbent (see eqn. 5). In the case of highly bioselective adsorbents, it is quite possible that the chemical processes could define the overall rate limiting step for achieving interphase equilibrium. It should be noted that the solution phase measurements[27,28] of the dissociation rate

TABLE II

EVALUATION OF NON-KINETIC CONTRIBUTION TO TOTAL PLATE HEIGHT ON 10-μm PARTICLES

Column: 5.0 × 0.5 cm I.D.; 27 mg Con A per gram silica, 10 μm, nominal pore size 500 Å. Mobile phase: pH 6.0, 0.02 *M* sodium phosphate, 0.5 *M* sodium chloride, 0.01 *M* magnesium chloride, 0.001 *M* calcium chloride. Solute: 0.2 m*M* pNp-galactoside, 25 μl injected.

Flow-rate (ml/min)	$H_{non\text{-}binding}$ *(mm)*		
	Calculated (k' = 0)*	*Calculated* (k' = 5)*	*Experimental*
0.2	0.068	0.073	0.077
0.4	0.077	0.087	0.097
1.0	0.091	0.12	0.12

* Calculated using eqns. 2–4 with $k_0 = 0.6$, $\gamma = 0.6$, $\lambda = 7.5$, $\omega = 2.7$, $\kappa = 0.167$, $\theta = 1.0$ and $D_m = 0.45 \cdot 10^{-5}$ cm²/sec.

of pNp-mannoside from Con A are on the order of 10 sec^{-1}. This should be compared with the diffusion time constant for a 10-μm particle (D_m/d_p^2) which is quite comparable, based on a diffusion coefficient of 10^{-5} cm^2/sec.

The apparent first order dissociation rate constants for the present system were evaluated by use of the equations developed by Horváth and Lin[10]. In order to estimate the non-chemical kinetic contributions to *H* two approaches were taken. In the first, we simply assumed that the *H* of a "binding" sugar would be equal to the sum of the *H* for a "non-binding" sugar of the same molecular weight and similar chemical structure and the *H* due to slow chemical kinetics; thus

$$H_{binding} = H_{non\text{-}binding} + H_{kinetic} \quad (21)$$

We then computed k_d from eqn. 5. In the second approach, we estimated the various structural packing parameters from typical literature data for spherical silica particles

TABLE III

EFFECT OF PARTICLE DIAMETER ON APPARENT DISSOCIATION RATE CONSTANT OF CON A–pNp-MANNOSIDE COMPLEX

Mobile phase: pH 6.0, 0.02 *M* sodium phosphate, 0.5 *M* sodium chloride, 0.01 *M* magnesium chloride, 0.001 *M* calcium chloride. Flow-rate: 1 ml/min.

Concentration injected (mM)	k_d *(sec⁻¹)**	
	d_p *= 10 μm***	d_p *= 50 μm****
0.1	0.32	0.34
0.2	0.33	0.31
0.4	0.23	0.21

* Calculated using eqn. 5.

** Column: 5.0 × 0.5 cm I.D.; 27 mg Con A per gram silica; nominal pore size, 500 Å.

*** Column: 5.0 × 0.3 cm I.D., 38 mg Con A per gram silica; nominal pore size, 420 Å.

to obtain an estimate of $H_{\text{non-binding}}$ using eqns. 2, 3 and 4. Both approaches give the same $H_{\text{non-binding}}$ within 11% (see Table II). Regardless of the approach taken to account for $H_{\text{non-binding}}$, it must be noted that on 10-μm particles, the H_{kinetic} term was by far the dominant (greater than 80%) contribution to the observed H, and therefore, errors in estimating non-kinetic term by either approach are not crucial. As indicated in Table II, the non-kinetic contributions to H are not strongly dependent on k'. Finally, the accuracy of the corrections for non-chemical effects is demonstrated by the fact that the k_d values obtained on both 10-μm and 50-μm particles are in good agreement (less than 10% difference; see Table III).

Effect of temperature and mobile phase modifiers on k_d

Since the peak widths in this system are so strongly influenced by the slow dissociation rates, we investigated the effect of three convenient variables on k_d. As shown in Fig. 7a, temperature has a marked effect on the observed rate constant. The apparent activation energy obtained from the slope of Fig. 7a for the dissociation on pNp-mannoside from Con A is 12.2 ± 1 kcal/mole. This agrees well with the solution phase estimate[28] of 16.8 ± 0.2 kcal/mole. Note that the apparent activation

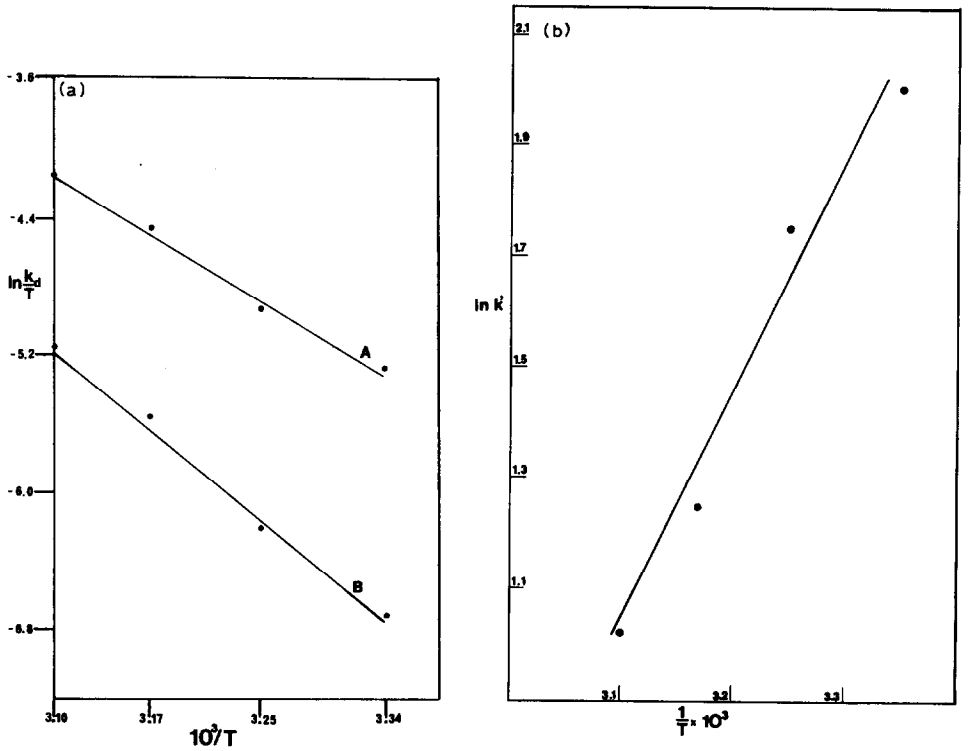

Fig. 7. (a) Temperature dependence of apparent dissociation rate constants. Column: 5.0 × 0.5 cm I.D.; 27 mg of Con A per gram of silica; 10 μm; nominal pore size, 500 Å. Mobile phase: pH 6.0, 0.02 *M* sodium phosphate, 0.5 *M* sodium chloride, 0.01 *M* magnesium chloride, 0.001 *M* calcium chloride. Flow-rate: 1 ml/min. Injection volume: 25 μl. Solutes: 0.1 m*M* pNp-glucoside (A); 0.1 m*M* pNp-mannoside (B). (b) Temperature dependence of k' of 0.1 m*M* pNp-mannoside.

TABLE IV

ACTIVATION AND THERMODYNAMIC PARAMETERS FOR THE DISSOCIATION OF THE CON A-pNp-MANNOSIDE COMPLEX

Mobile phase: pH 6.0, 0.02 *M* sodium phosphate, 0.5 *M* sodium chloride, 0.01 *M* magnesium chloride, 0.001 *M* calcium chloride. Temperature, 25°C.

$\Delta H^{\ddagger}$ (kcal/mole)	$\Delta S^{\ddagger}$ (e.u.)	ΔH^0 (kcal/mole)	ΔS^0 (e.u.)	Reference
12.2 ± 1	−19.2 ± 1	− 8.9 ± 1	−10.5 ± 1	t.w.*
16.8 ± 0.2	1.3 ± 0.7	− 7.3 ± 0.2	− 6 ± 0.7	28**
19.1 ± 1	10 ± 3	−12.8 ± 1	−23 ± 3	27**

* This work.

** Ionic strength = 0.3 *M*, pH 6.0.

energy is well in excess of that usually observed for the equivalent temperature coefficient of chromatographic mass transfer processes. Our observed rate constants are considerably smaller than those obtained in solution. This now appears to be due more to an entropic effect than due to a change in enthalpy upon forming the activated complex. Lewis *et al.*[28] have measured $\Delta S^{\ddagger}$ for this process as 1.3 ± 0.7 e.u. In contrast, we find $\Delta S^{\ddagger}$ to be −19.2 ± 1 e.u. for the two phase system. Unfortunately, the temperature effect on k_d is not large enough so that at reasonable temperatures (less than 50°C), the dissociation process will become fast enogh to make H_{kinetic} unimportant. Within this temperature range, the solute dissociation process is still appreciably slow compared with the rate of mass transfer. In addition, the sample k' values decrease considerably as the temperature is increased (see Fig. 7b). The ΔH^0 value for this process, as obtained from the slope of Fig. 7b, is −8.9 ± 1 kcal/mole. A comparison of the solution phase and two phase activation and thermodynamic parameters is given in Table IV.

A second convenient variable investigated as a means to increase the rate of solute dissociation was the concentration of competing sugar (αMDM) in the mobile phase. The results are shown in Fig. 8 and Table V. A very striking observation here is that k_d varies linearly with the mobile phase concentration of competing sugar. Thus, αMDM seems to promote elution both thermodynamically and kinetically. It is also evident that the dissociation rate in the absence of αMDM is not zero. These results, which are the first HPLC study of slow biochemical dissociation rates, must be compared to the analogous solution phase processes. Unfortunately, the literature data are quite varied on the effect of competing sugar on ligand debinding kinetics. For example, Lewis *et al.*[28] and Farina and Wilkins[27] indicate that the dissociation rate of pNp-mannoside from soluble Con A is not enhanced by the presence of competitor. In contrast, Podder *et al.*[29] find that the dissociation rate constant of RC_1, a protein, from Con A is increased in proportion to the concentration of competing sugar. From the results obtained in this study we infer that S_2 forms, at least transiently, an intermediate ternary species which more readily dissociates to liberate S_1 than does the simple Con A–S_1 complex. Once again, the increase in k_d is accompanied by a severe decrease in k' (see Table V). The addition of αMDM to the mobile phase affects the k' of pNp-mannoside more drastically than it does the plate height.

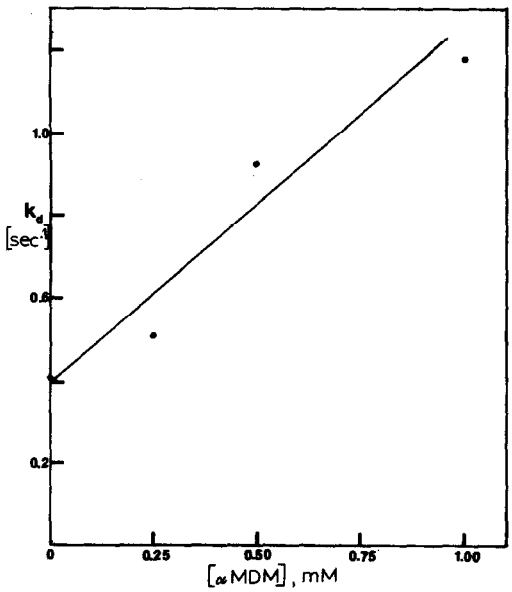

Fig. 8. Effect of competing ligand (S_2) on k_d of 0.05 m*M* pNp-mannoside. Column: 5.0 × 0.5 cm I.D.; 27 mg of Con A per gram of silica; 10 μm; nominal pore size, 500 Å. Mobile phase: pH 6.0, 0.02 *M* sodium phosphate, 0.5 *M* sodium chloride, 0.01 *M* magnesium chloride, 0.001 *M* calcium chloride. Injection volume: 25 μl. k_d calculated using eqn. 5.

We are currently investigating the use of other competing sugars.

As a final probe of the system, we investigated the effect of a low concentration (10%, v/v) of ethylene glycol on the chromatographic characteristics of the Con A columns. As shown in Table VI, the k' value decreased by nearly a factor of two, the k_d values were enhanced, but there was little overall improvement in H, partly due to the high viscosity of the solution. Estimates of the change in solute diffusion

TABLE V

EFFECT OF MOBILE PHASE COMPETITOR (αMDM) ON THE CHROMATOGRAPHIC PROPERTIES OF pNp-MANNOSIDE

Column: 5.0 × 0.5 cm I.D., 27 mg Con A per gram silica; 10 μm; nominal pore size, 500 Å. Mobile phase: pH 6.0, 0.02 *M* sodium phosphate, 0.5 *M* sodium chloride, 0.01 *M* magnesium chloride, 0.001 *M* calcium chloride. Flow-rate: 1 ml/min. Solute: 0.05 m*M* pNp-mannoside, 25 μl injected.

	Concentration of αMDM in mobile phase (mM)			
	0	*0.25*	*0.50*	*1.00*
k'	8.0	2.8	1.6	0.93
H_{total} (m*M*)*	0.77	1.13	0.79	0.66
k_d (sec^{-1})**	0.41	0.50	0.92	1.18

* Calculated using eqn. 13.
** Calculated using eqn. 5.

TABLE VI

EFFECT OF ETHYLENE GLYCOL (10%, v/v) ON k', H, AND k_d

Column: 5.0 × 0.5 cm I.D.; 27 mg Con A per gram silica; 10 μm; nominal pore size, 500 Å. Mobile phase: pH 6.0, 0.02 *M* sodium phosphate, 0.5 *M* sodium chloride, 0.01 *M* magnesium chloride, 0.001 *M* calcium chloride. Flow-rate: 1 ml/min. Solute: pNp-mannoside, 25 μl injected.

Concentration injected (mM)	*No ethylene glycol*			*Ethylene glycol added*		
	k'	H (mm)*	k_d (sec^{-1})**	k'	H (mm)*	k_d (sec^{-1})**
0.05	8.5	0.84	0.36	4.1	0.99	0.56
0.10	8.2	0.88	0.35	4.0	1.04	0.47
0.20	7.8	1.13	0.27	3.7	1.27	0.39

* Total plate height; from eqn. 13.
** Calculated using eqn. 5.

coefficient based on the Wilke–Chang equation and the viscosity of ethylene glycol–water mixtures indicate that only a small change in H should occur (*ca.* 20%). We do not believe that the effect of ethylene glycol can be quantitatively accounted for as solely an effect on solute diffusivity. The significant effect of ethylene glycol does indicate the existence of a significant "hydrophobic" component to the interaction between Con A and pNp-mannoside and agrees with the observations of Loontiens *et al.*, who claim that the *p*-nitrophenyl group does increase the hydrophobicity of the parent sugar[30].

CONCLUSIONS

In this work, the biochemical selectivity of Con A was shown to be preserved upon immobilization on a silica matrix. The resultant chromatographic adsorbent was characterized by estimating the thermodynamic and kinetic parameters and these were shown to be analogous to the solution phase properties of Con A. However, some differences were encountered. For example, the dissociation rates were observed to be considerably slower than in solution and dependent upon the concentration of competing ligand. It may be that immobilized affinity ligands can serve as a more appropriate model of cell surface interactions than the solubilized ligand systems. We have shown that microparticulate silica gel does not inhibit mass transfer as seriously as do more conventional supports (*i.e.* agarose) for affinity chromatography. The use of first and second peak moments provides an extremely convenient experimental approach to the study of the thermodynamics and kinetics of biological interactions on these solid supports.

ACKNOWLEDGEMENTS

Financial support for A. J. M. was provided by Proctor and Gamble Company, 3M Company, the American Cancer Society (Grant IN-13), and the National Science Foundation (CHE 8217363).

REFERENCES

1 S. Ohlson, L. Hansson, P.-O. Larsson and K. Mosbach, *FEBS Lett.*, 93 (1978) 5.
2 P.-O. Larsson, M. Glad, L. Hansson, M.-O. Mansson, S. Ohlson and K. Mosbach, *Advan. Chromatogr.*, 21 (1982) 41.
3 V. Kasche, K. Buchholz and B. Galunsky, *J. Chromatogr.*, 216 (1981) 169.
4 C. R. Lowe, Y. D. Clonis, M. J. Goldfinch, D. A. P. Small and A. Atkinson, in T. C. J. Gribnau, J. Visser and R. J. F. Nivard (Editors), *Affinity Chromatography and Related Techniques*, Elsevier, Amsterdam, 1982, p. 389.
5 J. R. Sportsman and G. S. Wilson, *Anal. Chem.*, 52 (1980) 2013.
6 A. Borchert, P.-O. Larsson and K. Mosbach, *J. Chromatogr.*, 244 (1982) 49.
7 R. R. Walters, *J. Chromatogr.*, 249 (1982) 19.
8 G. L. Nicolson, in H. Bittiger and H. P. Schnebli (Editors), *Concanavalin A as a Tool*, Wiley, New York, 1976, p. 3.
9 G. N. Reeke, Jr., J. W. Becker, B. A. Cunningham, J. L. Wang, I. Yahara and G. M. Edelman, in T. K. Chowdhury and A. K. Weiss (Editors), *Concanavalin A*, Plenum, New York, 1975, p. 13.
10 Cs. Horváth and H. Lin, *J. Chromatogr.*, 149 (1978) 43.
11 J.-C. Chen and S. G. Weber, *Anal. Chem.*, 55 (1983) 127.
12 J. C. Giddings, *Dynamics of Chromatography*, Marcel Dekker, New York, 1965, p. 29.
13 R. J. Kvitek, J. F. Evans and P. W. Carr, *Anal. Chim. Acta*, 144 (1982) 92.
14 L. D. Bowers and P. R. Johnson, *Biochim. Biophys. Acta*, 661 (1981) 100.
15 R. F. Borch, M. D. Berstein and H. D. Durst, *J. Amer. Chem. Soc.*, 93 (1971) 2897.
16 B. A. Cunningham, J. L. Wang, M. N. Pflumm and G. M. Edelman, *Biochemistry*, 11 (1972) 3233.
17 M. Broquaire, *J. Chromatogr.*, 170 (1979) 43.
18 A. W. J. de Jong, J. C. Kraak, H. Poppe and F. Nooitgedacht, *J. Chromatogr.*, 193 (1980) 181.
19 E. Grushka, M. N. Meyers, P. D. Schettler and J. C. Giddings, *Anal. Chem.*, 41 (1969) 889.
20 G. S. Hassing and I. J. Goldstein, *Eur. J. Biochem.*, 16 (1970) 549.
21 I. J. Goldstein, C. E. Hollerman and E. E. Smith, *Biochemistry*, 4 (1965) 876.
22 G. Scatchard, *Ann. New York Acad. Sci.*, 51 (1949) 660.
23 G. Scatchard, J. S. Coleman and A. L. Shen, *J. Amer. Chem. Soc.*, 79 (1957) 12.
24 L. L. So and I. J. Goldstein, *Biochim. Biophys. Acta*, 165 (1968) 398.
25 J. Yariv, A. J. Kalb and A. Levitzki, *Biochim. Biophys. Acta*, 165 (1968) 303.
26 G. H. McKenzie and W. H. Sawyer, *J. Biol. Chem.*, 248 (1973) 549.
27 R. D. Farina and R. G. Wilkins, *Biochim. Biophys. Acta*, 631 (1980) 428.
28 S. D. Lewis, J. A. Shafer and I. J. Goldstein, *Arch. Biochem. Biophys.*, 172 (1976) 689.
29 S. K. Podder, A. Surolia and B. K. Bachhawat, *Eur. J. Biochem.*, 44 (1974) 151.
30 F. G. Loontiens, J. P. Van Wauwe, R. DeGussem and C. K. DeBruyne, *Carbohydr. Res.*, 30 (1973) 51.